FROM SOURCE TO SURFACE: AN INVESTIGATION OF MAGMATIC LUNAR VOLATILES. Z. E. Wilbur[1], J. J. Barnes[1], S. A. Eckley[2,3], M. Brounce[4], S. J. Pomeroy[5], C. A. Crow[5], J. W. Boyce[6], J. L. Mosenfelder[7], T. J. Zega[1], and the ANGSA Science Team[8]. [1]Lunar and Planetary Laboratory, University of Arizona, Tucson, AZ, 85721, USA (zewilbur@email.arizona.edu); [2]Jacobs- *JETS*, NASA Johnson Space Center, Houston, TX, 77058, USA; [3]University of Texas, Austin, TX, 78712, USA; [4]University of California, Riverside, CA, 92521, USA; [5]University of Colorado, Boulder, CO, 80309, USA; [6]NASA Johnson Space Center, Houston, TX, 77058, USA;[7]University of Minnesota Minneapolis, MN, 55455, USA; [8]List of co-authors includes all members of the ANGSA Science Team (https://www.lpi.usra.edu/ ANGSA /teams/).

Introduction: Lunar missions led by NASA discovered water ice on the Moon's surface [1-3], revolutionizing views of the abundance, distribution, and potential sources of H_2O and other volatiles. Volatiles play an important role in affecting the rheological properties of minerals and melts and influencing magma eruption processes. In order to determine the indigenous volatile inventory of the Moon, it is vital to identify the magmatic and secondary processes that may have affected the volatile contents in lunar minerals [4].

As part of the Apollo Next Generation Sample Analysis (ANGSA) program we are investigating the petrogenesis of a set of four Apollo lunar basalts collected from the rim of Steno Crater 71035, 71037, 71055, and specially curated sample 71036. Our team is studying the petrology in 2D and 3D (this work), chronology (Pomeroy et al., LPSC 2022), oxidation state of sulfur in apatite (Brounce et al., LPSC 2022), and volatile inventory of the sample set in order to understand the age and genetic relationships among the basalts, their magma ascent conditions and eruptive signatures, and their degassing and surface histories.

Here we present the first detailed study of the 2D and 3D mineralogy, textures, 3D vesiculation, and chemistry of these basalts to shed light on their magmatic, volcanic, and post-eruptive histories.

***Figure 1**. Photograph of rock sample 71036,0. Apollo Photo S73-15675, credit: NASA JSC curation.*

Samples: Samples 71035, 71037, and 71055 were stored at "ambient" temperatures since their return to Earth in 1972. The newly released rock sample 71036, however, was stored at -20 °C (frozen) within one month of its arrival on Earth.

Prior studies of the Steno Crater basalts have shown that they are high-titanium (high-Ti) type and vesicular (20-40 vol.%) [5]. Some vesicles or vugs contain minerals (Fig. 1) [5]. The trace element chemical composition of the ambient samples suggests they are type B basalts [6]. Texturally they are fine to medium-grained, porphyritic, and plagioclase-poikilitic (Fig. 2, 3). The major mineral phases include olivine, pyroxene, plagioclase and ilmenite, with accessory phases of tranquillityite, baddeleyite, K-feldspar, apatite, merrillite, residual glass, and troilite (Fig. 2). Most of these samples lack exposure ages, and [7] determined a Rb-Sr age of 3.56 ± 0.09 Ga for 71055.

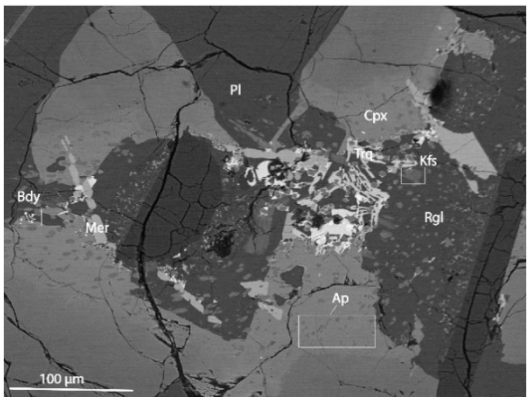

***Figure 2**. Backscattered electron image of 71055, major and accessory phases. Ap= apatite, Rgl= residual glass, Bdy = baddeleyite, Trq= tranquillityite, Cpx= clinopyroxene, Mer= merrillite, Kfs= K-feldspar, Pl= plagioclase.*

Methodology: X-ray elemental and BSE mapping of existing, polished thin sections and newly created thick sections of 71035, 71037, and 71055 were performed at NASA's Johnson Space Center (JSC) using the JEOL 7600F scanning electron microscope (SEM) and at the University of Arizona (UA) using the Cameca SX100 electron microprobe, respectively. The chemistry of olivine, pyroxene, ilmenite, feldspar, mesostasis glasses, and trace minerals like apatite (Fig. 2) within these samples was determined using the Cameca SX100 at UA. 2D modal mineralogy was determined from the X-ray maps using *ImageJ* software (Fig. 3). For 3D study, bulk subsamples of 71035, 71037, and 71055 were scanned using micro-X-ray computed tomography (μXCT) with the Nikon XTH 320 instrument at JSC to determine 3D mineralogy, fabrics, and vesiculation textures. The samples were

scanned with a 180 kV stationary and 225 kV rotating reflective target source and 1-2 mm Cu filter using the following range of conditions: 110-145 kV, 97-208 µA, and a voxel size range of 7.63-22.44 µm. These scans have been reconstructed using CT Agent Pro and visualized using Dragonfly™ software. Vesicles were separated and measured with Blob3D, and vesicle fabrics were quantified using Quant3D [8].

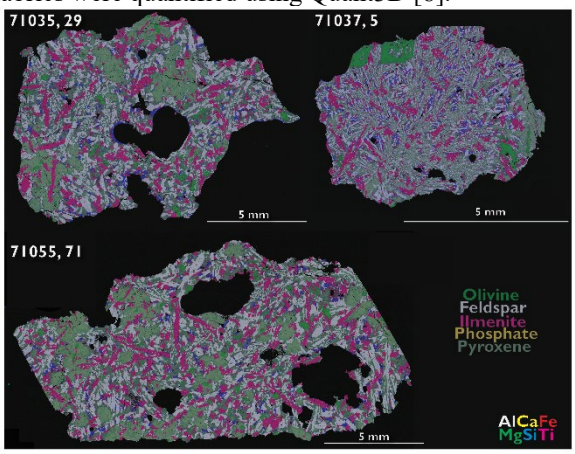

Figure 3. *Composite elemental maps of 71035, 71037, and 71055 with Fe in red, Mg in green, Si in blue, Al in white, Ti in magenta, and Ca in yellow.*

Results and Discussion: Micro-XCT offers a nondestructive means of analyzing the interior of a sample. Our µXCT results on 71035, 71037, and 71055 enabled determination of 3D modal mineralogy and vesicle abundances and textures. In 3D, phases of similar greyscale values presented challenges for segmentation. These phases are grouped and compared to 2D modes. The combined olivine + pyroxene volume percentage for the three samples (38.5 to 57.3 vol.%) spans and exceeds the range obtained from 2D analyses of thin sections (35 to 47.8 vol.%). Similar totals are observed for the feldspar, glass, and silica phases in 2D (30.5 to 43.7 vol.%) and 3D (25.8 to 47.1 vol.%). In comparison, ilmenite observed in 2D composes 17.3 to 27.4 vol.% compared to 11.3 to 19.3 vol.% in 3D. The high-Z phases (metal and sulfides) comprise a smaller proportion of the samples in 3D (0.002 to 0.1 vol.%) than in 2D (0.2 to 1.2 vol.%). Overall, the mineral modes are comparable between 2D and 3D datasets, and discrepancies could be attributed to modal mineralogy that is assumed to be volume percentages in 2D compared to actual 3D volumes.

Vesicle volume percentages were previously estimated from the Lunar Receiving Laboratory photographs and were found to range 20 to 40 vol.% for the studied samples. In 3D, we find 5.5 to 14.9 vol.% vesicles, which provides a lower limit of the vesiculation within the rocks, as vesicles impinging the exterior of each sample were excluded from our calculations, as well as vesicles below the scanning resolution.

We have isolated 59 to 549 vesicles per individual subsample, which were measured for their volumes and sphere-equivalent diameters in Blob3D. The orientations of the primary axes in the subsamples are widely distributed, and a preferred orientation is mild. The calculated strength parameter, C, is low for each volume ($C < 1$), and the shape factor, K, differs for each sample. All volumes display a cluster distribution ($K > 1$) along the primary and tertiary axes. Further fabric analysis using Quant3D yields similar results to those from Blob3D, and gives agreement among the primary, secondary, and tertiary eigenvalues. We observe a mild preferred orientation ($\tau1 > \tau2 > \tau3$) of the voids. We observed a limited sample set of vesicles in 2D, whereas the 3D scans provide hundreds of vesicles from which to separate and extract data to form a more complete picture of void space volumes, shapes, and fabrics.

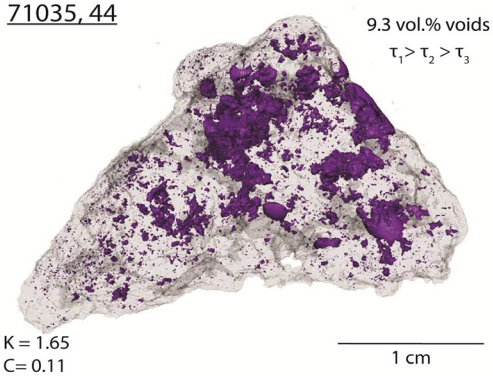

Figure 4. *The vesicles within 71035, 44 exhibit a mild preferred orientation with complex vesicle textures formed through the coalescence of 3 or more bubbles.*

We observed diversity in pore texture among the samples, which were collected from the same boulder on the Moon. Through the investigation of vesicle morphologies similar to those reported by [9], we will better understand the eruption histories of the Apollo 17 basalts. Moreover, coupling 3D data with 2D thin section modal mineralogy and chemical measurements will provide us with a more holistic view of the basalt petrogenesis.

Acknowledgments: We thank CAPTEM for the loan of lunar samples. Loan Le and Timmons Erikson are thanked for SEM mapping of Apollo thin sections. Ken Domanik is thanked for EPMA assistance. This work is partially funded by NASA Grant 80NSSC19K0803.

References: [1] Clark R.N. (2009) *Science,* 326, 562-564 [2] Pieters C.M. et al. (2009) *Science*, 326 (5952), 568-572 [3] Sunshine J.M. et al. (2009) *Science*, 326 (5952), 565-568 [4] McCubbin F.M. et al. (2015) *Am. Min*., 100 (8-9), 1668-1707 [5 Meyer (2011) Lunar Sample Compendium [6] Neal C.R. and Taylor L.A. (1993) Catalog of Apollo 17 Rocks, Vol. 2 [7] Tera F. et al. (1994) *EPSL*, 22, 1-21 [8] Ketcham R.A. (2005) Journal of Structural Geology, 2 (1217–1228) [9] Berg S.E. et al. (2006) *Bull Volcanol*, 78, 85-97.